Alexandre Jousse

in completion of the requirements for the Master of Science degree
in Nuclear Engineering of the Grenoble National Engineering School of Physics

Tritium transport in very high temperature reactors for hydrogen production

University of California, Berkeley
Department of Nuclear Engineering
Report UCBTH07-005
August 31, 2007

Research advisor: Per F. Peterson

University of California at Berkeley
Department of Nuclear Engineering

Table of contents

I. Introduction

1. Hydrogen futures

The production of liquid fuels from heavy oils, tar sands and biomass is expected to peak in the next decades. But it would require massive quantities of hydrogen **[14, 15]**.

Nuclear energy can be used to produce hydrogen. The avoidance of greenhouse gases emission and the large scale production possibility are the two major advantages of nuclear energy.

The most efficient methods to produce hydrogen require high temperature heat (700 to 950℃). Thermochemical cycles (sulfur-iodine (S- I) process) and high-temperature electrolysis (HTE) are the two major candidates.

To produce hydrogen in a highly efficient manner, the Next Generation Nuclear Plant (NGNP) project seeks to develop and demonstrate the feasibility of high temperature nuclear reactors (the nuclear reactor coolant temperature must be yet higher than the process temperature).

2. High temperatures reactors for hydrogen production

i. The Very High Temperature Reactor (VHTR)

There has been a recent resurgence of interest for helium cooled high temperature reactors. For instance, the Pebble Bed Modular Reactor is planned to be built in South Africa and the General Atomics GT-MHR are designs currently considered.

The Department of Energy (DOE) has selected the helium-cooled Very High Temperature Reactor (VHTR) for the NGNP project. It is the only near-term Generation IV concept that has the capability to provide process heat at high enough temperatures for highly efficient production of hydrogen.

The VHTR is a graphite moderated helium cooled reactor. It is a nominally 600 MW_{th} core connected to an intermediate heat exchanger for the delivery of process heat. The reactor can be a prismatic block core or a pebble bed core. For hydrogen production, the system supplies heat that could be used efficiently by the thermochemical S-I or HTE processes.

The VHTR will use the similar fuel as that used in the GT-MHR (the TRISO particle; Fig. 1). Uranium oxycarbide kernels with a diameter of 0.35 mm are coated with multiple layers of carbon and silicon carbide to form a 0.8 diameter microspheres. This fuel prevents release of radionuclides at very high temperature.

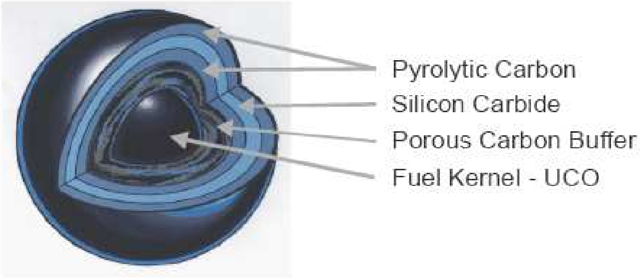

Fig. 1: The coated fuel particle (the TRISO particle)

In the prismatic block design, the coated particles are incorporated into a compact graphite-matrix fuel which, in turn, is loaded into a large graphite hexagonal block fuel assembly. Alternatively the coated particles can be incorporated into graphite pebble fuels.

ii. The Advanced High Temperature Reactor (AHTR)

As a longer-term alternative to gas cooled reactors, the Advanced High Temperature Reactor (AHTR) is a thermal 2400 MW_{th} that uses the same TRISO coated particle fuel in a liquid fluoride salt coolant.

Using liquid salt as a primary coolant provides several advantages, as well as new challenges. At operating conditions, liquid salt heat transfer properties are similar to those of water (appendix 1) and their high boiling point (>1300ºC) permits operation at temperatures that are only limited by material constraints. The low pressure (~1 bar) and chemically nonreactive coolant also greatly reduces the potential for pressurization over the reactor containment building and provides an important additional barrier for fission product release. Thus, the AHTR has several advantages over gas cooled systems. In comparison to the VHTR, the higher power output for a similar sized reactor vessel significantly improved economics (see appendix 3).

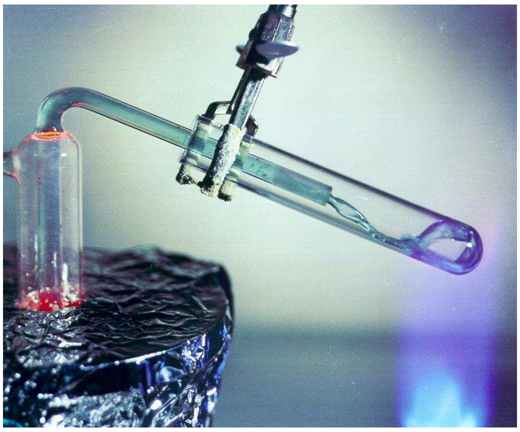

Fig. 2: The transparent liquid flibe flowing into a test tube in air

Flibe (Li_2BeF_4; Fig. 2) is a good candidate as a primary coolant due to its superior heat transfer capabilities. This salt won't be used in the intermediate loop because it is very expensive and contains beryllium. For the intermediate loop, we plan to use flinak, which is a ternary eutectic mixture of LiF, NaF, and KF. In the VHTR, the use of flinak in the intermediate loop is also studied.

The pebble bed fuel geometry is currently studied at UCB **[11]**. It shares the same TRISO particles with the hexagonal blocks fuel. They are embedded in a graphite matrix to obtain a 2.5 cm radius spherical fuel zone, which is protected by a 0.5 cm thick coating of graphite. The resulting pebbles are assembled into a randomly packed bed. The pebble bed option provides a more flexible refueling approach, but the release of fission radionuclides in the coolant will be larger in this design than in the prismatic one.

In the AHTR, the most important technical challenges are the control of corrosion by the liquid salts **[4]**, the freezing protection due to the high melting temperature of the salt (459℃ for flibe) and the thermal control approach, which must maintain the vessel and other components within an acceptable temperature range during transients and accidents. This topic is currently studied at UCB.

3. Tritium issue – Objective of this study

In these reactors, an intermediate transport loop is required to transport heat from the reactor core to the hydrogen plant. We plan to use a compact heat exchanger between the primary and the secondary coolants: the Intermediate Heat Exchanger (IHX; Fig. 3). The designs parameters of the exchanger are provided in Appendix 4. Between the secondary coolant and the hydrogen production system a second compact exchanger will be used: the Process Heat Exchanger (PHX). The secondary coolant may be either high pressure helium, or a low pressure liquid salt like flinak (LiF, NaF, KF).

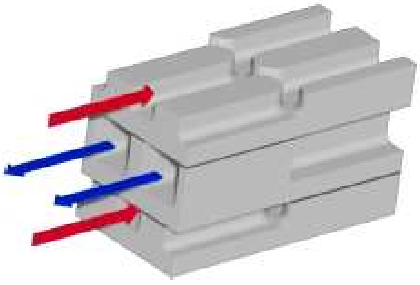

Fig. 3: Unit cell of a He to LS Intermediate Heat Exchanger (IHX)

The major issue for tritium transport is that at high temperatures materials can have high permeability to tritium. Therefore, tritium could contaminate hydrogen. Unlike high temperature metals, silicon carbide (SiC) has low permeability to tritium even at high temperature. This material will likely be used in the PHX to further reduce hydrogen contamination by tritium. But some additional studies are necessary to evaluate the effectiveness of this tritium permeation barrier and to identify tritium control strategies.

The objective of this work will be to evaluate the tritium permeation in the high temperature reactors (VHTR and AHTR) and finds appropriate solutions to reduce the contamination of hydrogen to remain within regulatory requirements.

II. Tritium transport model

1. Tritium production rate

In graphite moderated high temperature reactors, tritium is produced by ternary fissions and by activation reactions with graphite impurities (^{6}Li) or with control materials (^{10}B). Tritium is also provided by activation reactions with nuclides which are present in the coolant (^{3}He for the VHTR and ^{6}Li for the AHTR).

i. Tritium production by ^{3}He in the primary loop of the VHTR

^{3}He produces tritium by the following reaction: $^3He + n \rightarrow ^3H + p$

The thermal (n,p) cross section for ^{3}He is **σ_{He}=5.3x10^3 barns [13]**. The following equations give the evolution of tritium amount N_T in function of time:

$$\frac{dN_T}{dt} = \sigma_{He}\phi_{He}N_3 - \lambda N_T$$
$$\frac{dN_3}{dt} = -\sigma_{He}\phi_{He}N_3$$

where, N_3 is the amount of ^{3}He, λ=1.83 10^{-9} s^{-1} is the tritium decay constant and ϕ_{He} is the thermal neutron flux in helium.

To estimate the average thermal neutron flux in the helium coolant, we have to multiply ϕ_{core} by the ratio between the mass of helium in the core and the total mass in the core and primary loop.

The average thermal neutron flux in the core of the VHTR is approximately ϕ_{core} =2.5x10^{14} neutrons.cm^{-2}.s^{-1} **[12]**.

The power density in the core of the VHTR is 6.6 MW$_{th}$.m^{-3} **[12]**. The thermal power is 600 MW$_{th}$. Consequently, the volume of the core is about 90 m^3. The coolant void fraction is approximately 10 %. Thus, we deduce the volume of helium in the core: **V_{core}~80m^3**.

It is estimated that a GT-MHR requires a primary helium inventory of 14.3 kg per MW$_e$. Thus, a 265 MW$_e$ GT-MHR contains about 3.8x10^3 kg of helium. The amount of helium in the primary loop of a VHTR is considered to be the same. We estimate the volume of Helium in the primary loop: **V_{He}~1200 m^3** (we use the ideal gas law with T=1000℃ and P=7 MPa).

Therefore, the average thermal neutron flux in the helium coolant is **ϕ_{He} =1.7x10^{13} neutrons.cm^{-2}.s^{-1}** (ϕ_{He}= $\phi_{core}V_{core}/V_{He}$).

We deduce the half period for tritium production $T_p = \frac{\ln 2}{\sigma_{He}\phi_{He}} = 80 days$. It is far smaller than the tritium half life $T_{1/2} = \frac{\ln 2}{\lambda} = 12 years$, so tritium decay can be neglected.
Thus, the tritium amount produced by ^{3}He in the primary coolant of the VHTR is given by:

$$N_T(t) = N_0(1 - e^{-\sigma_{He}\phi_{He}t})$$

where, N_0 is the initial amount of ^{3}He in the reactor.

The natural abundance of ^{3}He is 0.000137 atom percent. Therefore, the VHTR initially contains about 5 g of ^{3}He. We can consider that **about 240 days after the start-up of the reactor**, we have produced **5 grams of tritium,** which corresponds to an activity of **A=1.8 10^{15} Bq =5x10^4 Ci**. This amount of tritium corresponds to a partial pressure of tritium molecules in the primary coolant of 6 Pa.

Moreover, if we consider a helium leakage rate of 10% per year, we can consider that we add 0.5g of ^{3}He each year. It corresponds to an **additional production rate of 5x10^3 Ci.yr^{-1}** (if we consider the production of tritium instantaneous which is false since for production T_p=80 days).

ii. Tritium production by ^{6}Li in the primary loop of the AHTR

^{6}Li produces tritium by the following reaction: $^6Li + n \rightarrow {}^3H + \alpha$

The thermal (n,α) cross section for ^{6}Li is **σ_{Li}=940 barns [13]**. The thermal neutron capture cross section of ^{6}Li is about 40 mbarns. Therefore, we can neglect the absorption and all the ^{6}Li will be transformed into tritium under sustained neutron irradiation.

The thermal neutron flux in the core of the AHTR is approximately ϕ_{core} =3.4x10^{14} neutrons.cm^{-2}.s^{-1}**[12]**. The power density in the core of the AHTR is 10.2 MW$_{th}$.m^{-3} **[12]**. The thermal power is 2400 MW$_{th}$. Thus, we deduce the core volume: V~235 m^3. For the pebble bed AHTR design, 40% of this volume is occupied by flibe (95 m^3) and the reminder by fuel. According to the current design, the volume of the primary coolant is about 130 m^3. Therefore, the average thermal neutron flux in the helium coolant is: **ϕ_{LS} ~2.5x10^{14} neutrons.cm^{-2}.s^{-1}.**

The comparison of $T_p = \frac{\ln 2}{\sigma_{Li}\phi_{LS}} = 34 days$ and $T_{1/2} = \frac{\ln 2}{\lambda} = 12 years$ leads to:

$$N_T(t) = N_0(1 - e^{-\sigma_{Li}\phi_{LS}t})$$

where, $N_T(t)$ is the tritium amount produced by ^{6}Li in the primary coolant of the AHTR and N_0 is the initial amount of ^{6}Li in the reactor.

The natural abundance of ^{6}Li is 7.5 percent. In the primary coolant we plan to use a flibe with 4 ppm of ^{6}Li. In the pebble bed AHTR, the total inventory of liquid salt in the primary coolant is 130 m^3. The mass density of the flibe is about ρ=1940 kg/m^3. Therefore there are about 21 mol of ^{6}Li in the primary coolant

Thus, **about 3 months after the start-up of the reactor, 63 g of tritium will have been produced in the primary coolant of the AHTR**. It corresponds to $6.3\text{x}10^{5}$ Ci.

We can notice that in flibe, ^{6}Li is produced by: ^{9}Be (n,α) ^{6}He $\longrightarrow$ (β decay) ^{6}Li. And then, tritium is produced by the same reaction: ^{6}Li (n,α) ^{3}H. The thermal neutron absorption cross section of ^{9}Be is low: $\sigma_{thermal}\sim 10$ mbarns (that's why we use beryllium as reflector and moderator). This reaction is not negligible with fast fission neutrons: $\sigma_{fast}\sim 1$ barns. We would need more information about the neutron flux of the reactor to evaluate the tritium production by ^{9}Be. But it is certainly smaller than the rate which is produced by the initial amount of ^{6}Li in the reactor (at least during the first year after the start-up of the reactor). Thus, we will neglect this reaction in this report.

iii.Tritium production rate by ternary fission

To calculate the tritium production rate by ternary fission, we use the fact that each fission produces 200 MeV. Therefore, for a 600 MW_{th} reactor (VHTR), we have 2.10^{19} fissions per second. Since the tritium emission probability for fission reactions induced by thermal neutron on ^{235}U is about 10^{-4} **[6]**, we deduce the tritium production rate: 0.3 $g.yr^{-1}$. It corresponds to an activity of $3\text{x}10^{3}$ $Ci.yr^{-1}$. In the 2400 MW_{th} AHTR, the tritium production by ternary fissions is 1.2 $g.yr^{-1}$. It corresponds to $1.2\text{x}10^{4}$ $Ci.yr^{-1}$.

To be released, tritium generated by fission reaction in the fuel kernel must diffuse from where it is generated to the coolant. Although the fuel prevents release of radionuclides, tritium releases are possible at very high temperature. But even if we consider that all the tritium produced by ternary fission permeates in the primary loop, its production rate will be at least one order of magnitude lower than the one directly produced by the coolant.

Therefore, we will only consider the tritium production by neutron absorption reactions on ^{3}He for the VHTR and on ^{6}Li for the AHTR. We will focus on tritium transport after the start-up of the reactor. In fact, this period is the worst for tritium production. We will consider that, if we are able to manage this problem during this period, we will also be able to manage it during all the life of the reactor.

2. Regulatory requirement

i. Flow of hydrogen

To calculate the maximal allowed tritium permeation flux through the PHX, it is indispensable to estimate the flow of hydrogen produced in the reactor.

Here is the fundamental equation for hydrogen production and its energy:

$$H_2O_{(g)} \rightarrow \frac{1}{2}O_{2(g)} + H_{2(g)} \text{ with } \Delta_r H = -\Delta Hf_{H20} \sim 250 \text{ kJ.mol}^{-1}$$

We consider that the thermal efficiency of hydrogen production (R) is 50%. Thus, we can deduce Q_{VHTR} the flow of hydrogen for the VHTR (P_t~600 MW):

$$Q_{VHTR} = \frac{RP_t}{\Delta_r H} \approx 1kmol.s^{-1} \approx 8 \times 10^4 m^3 (STP).h^{-1} \approx 6 \times 10^7 kg.yr^{-1}$$

For the AHTR, P_t~2400 MW:

$$Q_{AHTR} = \frac{RP_t}{\Delta_r H} \approx 4kmol.s^{-1} \approx 3.2 \times 10^5 m^3 (STP).h^{-1} \approx 2.4 \times 10^8 kg.yr^{-1}$$

ii. Harmless limit

Tritium is readily transported in the environment since it is exceedingly mobile as tritiated water. It has multiple pathways to humans: via inhalation and drinking water, through ingestion of food, and absorbed through the skin. In the human body, 80% of the atoms are hydrogen atoms, which can be replaced by tritium. That's why exposure to tritium must be carefully controlled and limited.

In the US, the legal limit for tritium in drinking water is 740 Bq/L. Hydrogen can be considered harmless if the water we would produce with this hydrogen by addition of oxygen is under this limit. This **harmless limit is 6 Bq/g of hydrogen** (=160 pCi/g of H_2). It corresponds to 1.6×10^{-14} g of T/g of H_2. This limiting value may be increased if the oxidized hydrogen is diluted in other water.

This regulatory limit is uncertain and could be modified in the future. After studies of tritium effects on environment, Canada, which has today one of the highest tritium legal limit for drinking water (7000 Bq/L), plans to reduce this limit to 20 Bq/L. Therefore, if we want to produce hydrogen in the next decades with nuclear energy, we will certainly have to reach a lower limit. Nevertheless, in this study, we will compare the results of our simulations with the clearly harmless limit, which has been calculated above (6 Bq/g).

Moreover, we also have to control the tritium, which is released in the environment. The amount of tritium that is acceptable to be released in environment during usual operation is 20 Ci/day **[5]**. Another important issue for tritium safety is potential exposures to workers in buildings. The permissible radioactivity in the air of working rooms is 3×10^5 Bq/m^3 (8.1×10^{-6} Ci/m^3) **[8]**.

We won't study these problems in this work. But the low regulatory values in comparison to the amount of tritium produced in the reactor show that a tritium removal systems is likely required. Nevertheless, we can notice that, even if we remove the tritium from the reactor, the problem of tritium storage still remains. In fact, it is very difficult to store it, and that's why nuclear industry generally dilutes its tritium wastes in environment. Heavy water reactors produce sufficiently large quantites of tritium that it is generally recovered from the heavy water moderator and coolant and stored [16]. But in the future it may become necessary to recycle tritium.

3. The lumped mass approximation

We can estimate the order of magnitude of the time to uniformly mix the primary coolant based on the time scale for one complete fluid transit through the primary loop.

For the VHTR: τ =m/Q=12 s where, m=$3.8\text{x}10^3$kg is the mass of helium in the primary loop and Q=$3.2\text{x}10^2$ kg.s^{-1} the mass flow **[7]**.

For the AHTR: τ =25s where, m=$2.3\text{X}10^5$kg and Q=$9.2\text{x}10^3$ kg.s^{-1} **[11]**.

For the secondary coolant, this time is longer since a parallel hot leg and cold leg piping is assumed to run 100 m in length between the IHX and the PHX. For instance, in the VHTR, for a He/LS IHX, τ =100s (m=10^5kg and Q=9.8 x10^2 kg.s^{-1} **[7]**).

Thus, we will consider that the forced convection allows rapid mixing, and consequently, we will assume that the concentrations of tritium are uniform in the primary and secondary coolants. Therefore our model will be zero-dimensional (e.g., a lumped mass approximation).

m_1 and m_2 are the mass of tritium respectively in the primary coolant and in the secondary coolant; m_3 is the total amount of tritium, which permeates through the PHX; m_p is the mass of tritium produced in the primary coolant. With this lumped mass approximation, the inventories of tritium can be calculated as a function of time using finite difference equations,

$$m_1(t)= m_p(t)+m_1(t-1)-S_1j_{12}(t)$$
$$m_2(t)= m_2(t-1)+S_1j_{12}(t)-S_2j_{23}(t)$$
$$m_3(t)= m_3(t-1)+S_2j_{23}(t)$$

where, j_{12} is the tritium flux from the primary coolant to the secondary coolant
j_{23} is the tritium flux from the secondary coolant to the hydrogen side
S_1 is the surface area of IHX (Intermediate Heat Exchanger)
S_2 is the surface area of the PHX (Process Heat Exchanger)

In the VHTR, the surface area for a helium/liquid salt IHX is 4100 m^2 and 3200 m^2 for a helium/helium IHX **[7]**. In the AHTR, the surface area of the IHX is 3500 m^2. For simplicity, we assume that these surface areas are the same for the PHX.

For the modeling, we have used a Matlab code (see appendix 5).

4. Tritium permeation regimes

i. Diffusion limited regime

Tritium transport through the metal or silicon carbide of a heat exchanger involves a series of processes. If there are substantial differences in the processes, the total transport is governed by the slowest step, or highest resistance, in the permeation process. We can assume first that the diffusion in the heat exchanger material is the limited regime. This means that the interactions of tritium molecular gas with metal (or SiC in the case of a He/He IHX) and the interactions of dissolved tritium in liquid salt with metal or SiC don't reduce the permeation flux. In that case, the tritium molecule T_2 flux is given by:

$$j_{1\rightarrow 2} = \frac{K\left(\sqrt{P_1} - \sqrt{P_2}\right)}{e}$$

where, K= DS is the T_2 permeability of the material, D and S are respectively the diffusity and the Sieverts' constant of the material, P_1 and P_2 are the partial pressures of tritium molecules (T_2) on each sides of the plate and e is the effective thickness of the plate. For the IHX and PHX a value of **e=1.6 mm** is used.

ii. Surface limited regime

The tritium transport becomes surface-limited when it is limited by the physico-chemical reactions of adsorption and recombination occurring at the surface of the heat exchanger material rather than by interstitial diffusion in the heat exchanger material.

Thin oxide films on the surface of the exchangers could result in a surface-limited regime. Another possibility, in the case of a He/LS IHX for the VHTR or in the AHTR, is that the permeation is limited by the desorption of tritium from the liquid salt to the exchanger surface. This effect could particularly be strong with flinak since tritium dissolves in it as atomic particles.

To simulate this regime, we would need the tritium adsorption and recombination constant **[5]**. But these parameters are strongly dependant of the experimental conditions and are consequently unknown for the system of interest here. Therefore, in first approximation, we will assume that the permeation flux is given by:

$$j_{1\rightarrow 2} = \frac{K\left(\sqrt{P_1} - \sqrt{P_2}\right)}{PRF \times e}$$

where PRF is the permeation reduction factor

The behavior of liquid salts with the IHX and PHX materials has been studied experimentally in corrosion testing, but the impact on tritium transport is unknown. But studies have already been done to understand the behavior of tritium with water facing materials for fusion applications **[10]**. It has been shown that the permeation of aqueous tritium through a metal was three orders smaller than that of gaseous tritium. Of course, the behavior of tritium in water is completely different than that in liquid salt (formation of HTO occurs in water whereas a pair H+F- is produced in the liquid salt); but the binding energy of tritium in liquid salt probably leads to the same type of permeation reduction. For this reason PRF values ranging between 10 and 1000 are studied here.

iii. Materials parameters

Here are the materials parameters we will need for our tritium transport study. Even if the IHX and PHX operate at below 1000℃ (~950℃), t he parameters are given at this temperature. It won't affect our tritium transport analysis since we will study the effects of the variation of these parameters. In fact, they will probably vary with experimental conditions.

Liquid fluoride salts have very low chemical reactivity with nickel based alloys (such as Hastelloy XR), that's why we plan to use nickel based alloy for the IHX.

**At 1000℃, the tritium molecule (T_2) permeability for Hastelloy XR is:
$K_{XR}=6.5\times10^{-10}$ mol.m^{-1}s^{-1}Pa$^{-0.5}$ [1]**.

At 1000℃, the T_2 permeability for SiC is: $K_{SiC}=2\times10^{-15}$ mol.m^{-1}s^{-1}Pa$^{-0.5}$ [3].
We will use this data for the PHX.

In the case of a helium/liquid salt exchanger, we also need the solubility of tritium in liquid salt. **At 1000℃, the solubility of hydrogen molecules (H_2) in Flinak is $S_{LS}=10^{-5}$ mol.m^{-3}Pa^{-1} [2]**. The concentration C_T of tritium is given by the Henry law: **$C_T= S_{LS}P_{T2}$**. We will assume that the solubility is the same for T_2 (it is probably smaller since the repulsive macroscopic surface tension is larger for tritium). Impurities in liquid could also modify the solubility. For example, hydrogen will probably diffuse through the PHX, and its presence will reduce tritium solubility in the salt.

If we choose another liquid salt, the tritium solubility would probably change since tritium behavior depends on the chemical species in the salt. The solubility of tritium in flinak is high in comparison to several other liquid salts including flibe. Studies have already been done on tritium transport in flibe for fusion applications. They show that at 500℃ the solubility of hydrogen is a thousand times lower than that of hydrogen in flinak **[9]**. A proposed explanation for this difference could be that hydrogen in flinak doesn't dissolve as a hydrogen molecule, whereas it is thought to be the case in flibe. The relatively good solubility of tritium in flinak means that it could provide a good tritium permeation barrier.

III. Tritium transport analysis

The following simulations are performed for just after the start-up of the reactor, which is the worst case for tritium production. We first study the tritium inventory without any tritium removal systems. Then, we will talk about the possible need for tritium removal to control the tritium inventory and concentrations.

We study the three envisaged designs: the VHTR with a helium intermediate loop, the VHTR with a liquid salt intermediate loop and the AHTR;

1. The VHTR with a helium intermediate loop

i. Diffusion limited regime

If we assume the diffusion limited regime (PRF=1), a significant part of the total amount of tritium (N_0~5g) has diffused in the hydrogen side of the reactor. In fact, after 600 days, almost 2 g of tritium have permeated through the Process Heat Exchanger (Fig. 4).

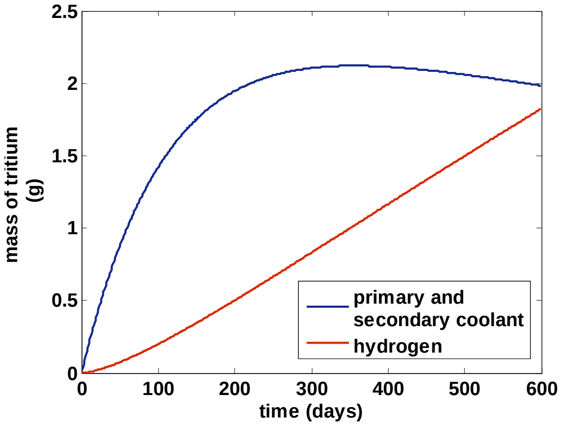

Fig. 4: Mass of tritium (g) in each system (He/He IHX; PRF=1)

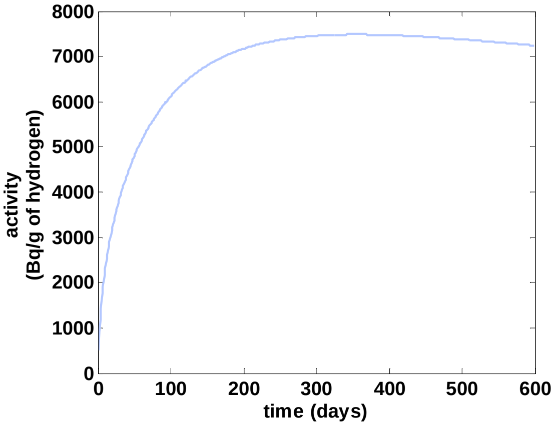

Fig. 5: Activity of hydrogen (Bq/g of H_2) (He/He IHX; PRF=1)

By considering the hydrogen flow (Q=1kmol.s^{-1} for the VHTR), we deduce the activity of hydrogen (Fig. 5). The average activity is approximately 6000 Bq/g of hydrogen. It is much larger than the harmless limit (6 Bq/g of H_2).

Here are some commentaries:

Fig. 4 shows that the amount of tritium is almost equal in the primary and in the secondary coolants. It comes from the fact that the steady state between the primary and the secondary coolant is fast. In fact, the time scale for tritium diffusion through the metal plate is only: $\tau = e^2/D_{XR}$ = 2 min. Therefore, tritium partial pressure in both coolants is equal (Fig. 6), and since we have assumed that the volumes of the primary and secondary coolant are the same, the amount of tritium is also the same.

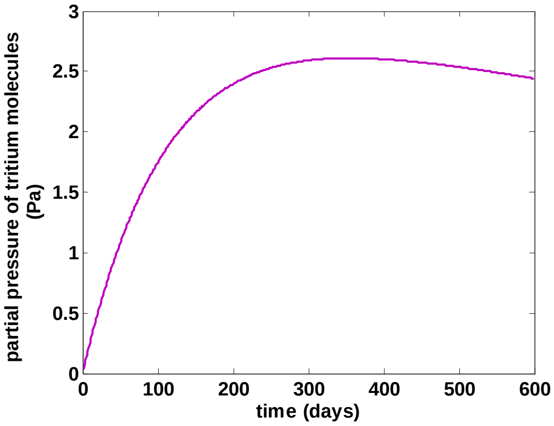

Fig.6: Partial pressure of tritium molecules in primary and secondary coolants (He/He IHX; PRF=1)

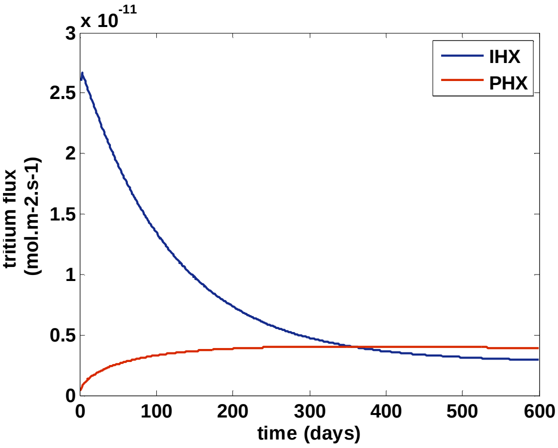

Fig. 7: Tritium fluxes in the IHX and in the PHX (He/He IHX; PRF=1)

Although the permeability for the IHX material (Hastelloy) is almost 10^5 bigger than that for the PHX (SiC), the fluxes of tritium in the IHX and in the PHX have the same order of magnitude (Fig.7).

To understand it, we have to compare the tritium fluxes j_{12} and j_{23} through the IHX and the PHX, respectively.

We have: $j_{12} = K_{XR}\frac{\sqrt{P_1}-\sqrt{P_2}}{e}$ with $\sqrt{P_1}-\sqrt{P_2} \approx 0$ (see explanation below)

At the same time, the partial pressure of tritium is negligible in the hydrogen generation system. That's why the flux in the PHX is given by the following equation: $j_{23} = \frac{K_{SiC}\sqrt{P_2}}{e}$

Since $K_{XR} << K_{SiC}$, it explains why the fluxes have the same order of magnitude.

ii. Surface limited regime

In the case of Helium/Helium exchanger, the formation of thin oxide films on the surface of the exchangers is the most important permeation reduction factor. These oxide films would probably reduce the thermal conductivity and therefore, we will certainly try to reduce to the maximum their formation in the exchangers. That's why, here, we only study the effect of a permeation reduction factor of 10.

With this hypothesis, the efficiency of the permeation barrier effect is stronger (Fig. 8). As expected, the effect is the reduction of hydrogen activity by a factor 10. During the first years after the start-up of the reactor, the average activity is 700 Bq/g of H_2 (Fig. 9).

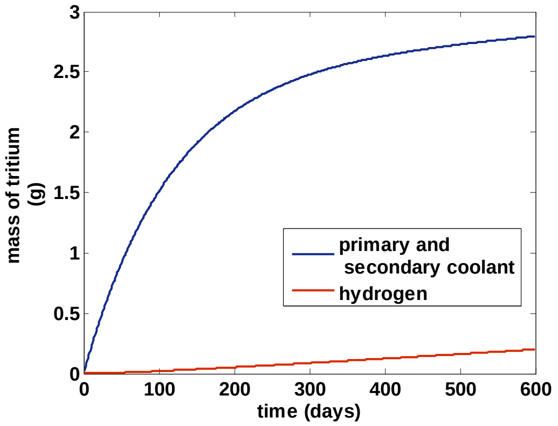

Fig. 8: Mass of tritium (g) in each system
(He/He IHX; PRF=10)

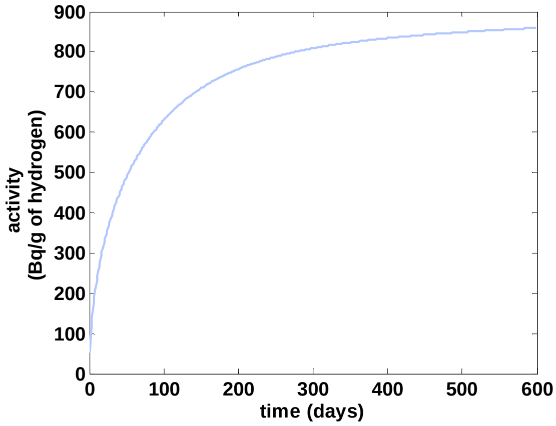

Fig. 9: Activity of hydrogen (Bq/g of H_2)
(He/LS IHX; PRF=10)

We have studied the effects of bigger permeation factors, and the simulations have shown some interesting behaviors. Only the modification of the permeability of the PHX (silicon carbide) has an influence. The modification of the permeability of the IHX by a factor 1000 doesn't change the results. It comes from the fact that even if the permeability of Hastelloy increases by a factor of 1000, the steady state between the primary and the secondary coolant would still be very fast.

We have also assumed that the permeability for silicon carbide was reduced by a factor 10 (Fig. 10).

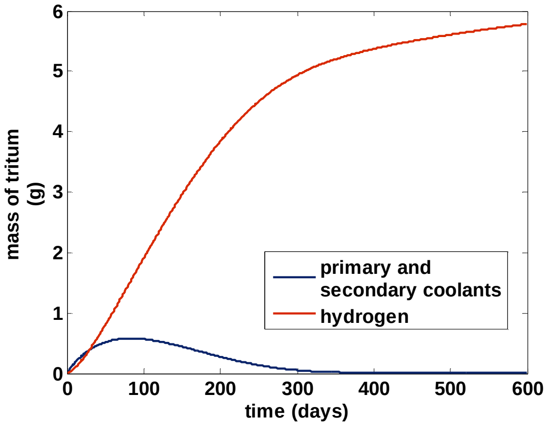

Fig. 10: Tritium mass in each system with the hypothesis
that we reduce SiC permeability by a factor 10

With this assumption, the SiC is not a tritium permeation barrier anymore. The tritium is almost diffused instantaneously to hydrogen. It proves the necessity to build the PHX with SiC (or another material with the same tritium permeability).

These simulations show that it would be very interesting to have a better understanding of the coolant/SiC interface.

2. The VHTR with a liquid salt intermediate loop

i. Surface limited regime

The feasibility of fluoride salt use as a heat exchange fluid for high temperature applications has been demonstrated **[4]**; there are some possible approaches to control corrosion and redox potential in fluoride salts. Nevertheless, in the case of a liquid salt exchanger, the surface effects could particularly be strong (for instance, the tritium desorption from the liquid salt to the exchanger). That's why, in the case of a Helium/Liquid Salt IHX, we study tritium transport with permeation reduction factors from 10 to 100.

Fig. 11 shows the tritium inventory for a permeation reduction factor equal to 10. The permeation barrier is efficient but not sufficient. For PRF=100, the activity of hydrogen is below 200 Bq/g (Fig. 12). But stronger surface effects of the liquid salts could be expected.

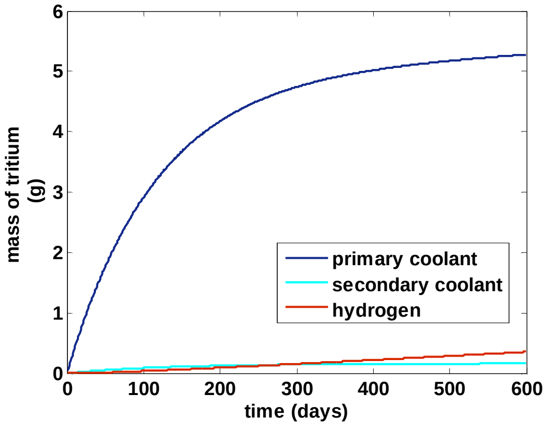

Fig. 11: Mass of tritium (g) in each system (He/LS IHX; PRF=10)

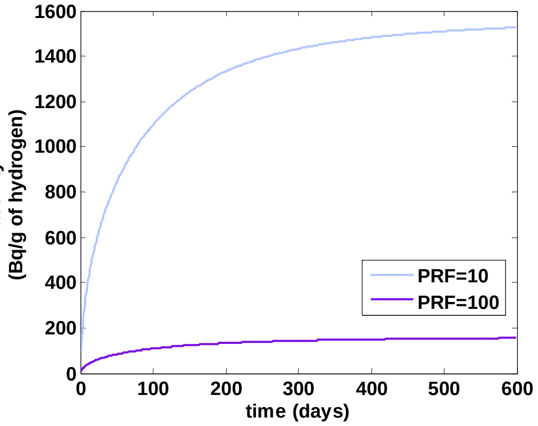

Fig. 12: Activity of hydrogen (Bq/g of H_2) (He/LS IHX)

In comparison to the He/He IHX (Fig. 9), for the same permeation reduction factor (PRF=10), the activity of hydrogen is larger. Since the tritium solubility in the liquid salt is low, very little tritium permeates in the intermediate loop. Therefore the tritium partial pressure is bigger (5 Pa instead of 2.5 Pa in He/He VHTR) and thus, the flux through the PHX is somewhat larger.

ii. Liquid salt solubility influence

We are studying the influence of the variation of the tritium solubility in liquid salt. The solubility of tritium in flinak is relatively high. But some impurities (especially hydrogen) could reduce it.

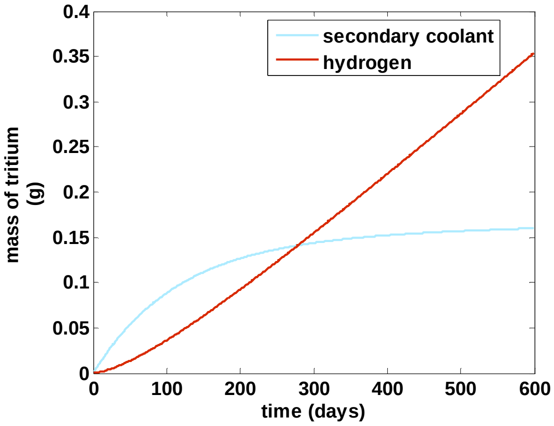

Fig. 13: Masses of tritium if there are no impurities in flinak (PRF=10)

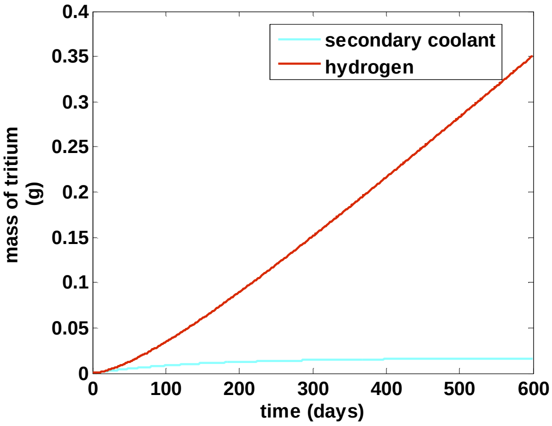

Fig. 14: Masses of tritium if there is some impurities in Flinak (ideal solubility divided by a factor 10; PRF=10)

Fig. 13 and 14 clearly show that, in the VHTR, the variation of liquid salt solubility does not influence the amount of tritium in hydrogen. In fact even if the solubility changes, the amount of tritium in the liquid salt is so small in comparison to the amount of tritium in the primary coolant (Fig. 11) that it has no influence on the partial pressure and consequently, no influence on the tritium permeation flux.

3. AHTR

Here is the tritium inventory in the AHTR with PRF=10 (Fig. 15). In this reactor, the primary and secondary coolants are liquid salts (130 m^3 and 50 m^3 are the volumes of the primary and secondary coolants, respectively).

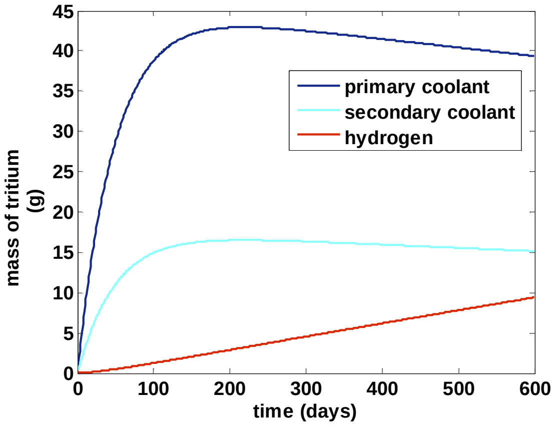

Fig. 15: Mass of tritium (g) in each system in the AHTR (PRF=10)

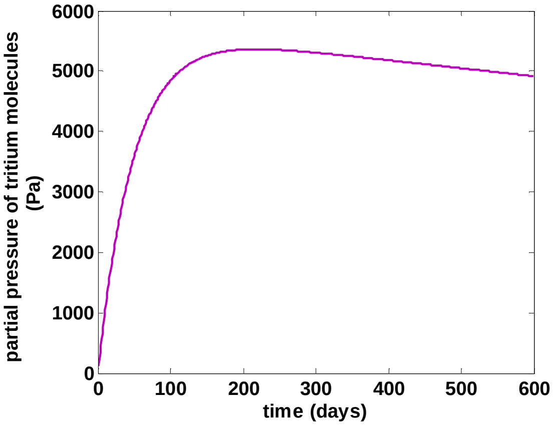

Fig. 16: Partial pressure of tritium molecules in primary and secondary coolants in the AHTR (PRF=10)

The tritium partial pressure is about one thousand time larger in this reactor than in the VHTR (Fig. 16): 5000 Pa instead of 5 Pa. This increasing comes from the low tritium solubility of the primary coolant. This high partial pressure makes it possible that a large fraction of the tritium production could be recovered through the primary salt cover gas system.

The consequence of this high partial pressure, if the tritium were not removed, is a high hydrogen contamination by hydrogen: if we consider a permeation reduction factor of 10, the activity of the hydrogen produced during the first years of the reactor would be 9000 Bq/g (Fig. 17 below). But the use of liquid salts in this reactor could lead to important surface's effect. If we assume PRF=1000, the activity of hydrogen would be 100 Bq/g. But, it is still above the harmless limit (6 Bq/g).

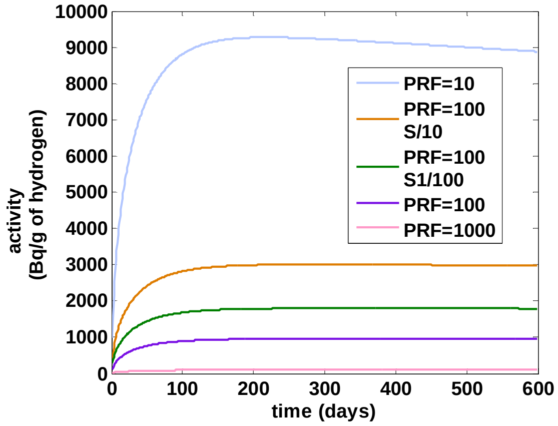

Fig. 17: Activity of hydrogen (Bq/g of H_2)
in the AHTR

We have also studied the effects of tritium solubility variations (a permeation reduction factor of 100 has been hypothesized). First, if we assume that both coolants have the same tritium solubility as flinak (which is high in comparison to other liquid salts), the hydrogen activity is A_1=1000 Bq/g (purple curve).

As we saw in the preceding section, impurities could reduce trititum solubility. If we assume that it is reduced by a factor 10 in both coolants, the hydrogen activity becomes A_2=3000 Bq/g (orange curve). Therefore, the variation of the liquid salt solubility has an influence in the AHTR. Contrary to the VHTR, its presence in the primary loop affects the tritium partial pressure in the reactor and thus in the absence of tritium recovery its diminution increases the contamination of hydrogen (We can verify that $A_2 \approx \sqrt{10} A_1$).

At last, the green curve represents the case where the solubility of the primary salt is one hundred times lower than the one of the secondary salt (clean flinak). This case is the most realistic. In fact, in the primary loop, we plan to use flibe which has low tritium solubility, whereas the use of flinak with relative high solubility is the most probable in the intermediate loop. In that case, the hydrogen activity is 1800 Bq/g. Therefore, in the case without tritium recovery the low tritium solubility of flibe in the primary loop could be compensated by the high one of flinak.

To conclude, we can notice that it would be very useful to know with accuracy the tritium solubility in the salts to predict with precision the tritium behavior in the AHTR.

4. The hot leg path

The liquid salt hot leg is assumed to be 100 m long between the IHX and the PHX. For liquid salts, the piping operates at the salt temperature and insulation is placed on the outside of the pipe. The high temperature in the metallic wall of the hot leg could present an important transport path for tritium into the insulation system surrounding the piping. This pathway is not expected in the helium piping because it has internal insulation and a much cooler outer wall that makes the metal relatively impermeable to tritium.

If we assume that there is a thin gas layer between the outside of the pipe and the insulation system, and if this gas layer is purged by a tritium removal system so the tritium partial pressure is small, then the tritium flow through the hot leg pipe wall is given by: $Q = 2\pi L \dfrac{K_{XR}\sqrt{P_2}}{\ln \dfrac{d_2}{d_1}}$

where, d_1=0.2 m is the pipe inside diameter and d_2=0.26 m is the pipe outside diameter.

We can notice that this gas layer is probably not thermally interesting (heat losses to the environment from the secondary heat transport system shall be limited to less than 1%); but the goal of this analysis is to study the possible efficiency of purging the hot leg insulation system for tritium removal.

i. VHTR

The study shows that one year after the start-up of the reactor almost all tritium has permeated through the hot leg (Fig. 18 and 19).

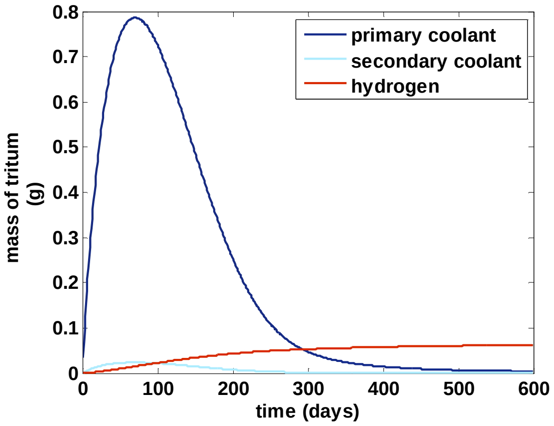

Fig. 18: Tritium masses in each system by considering the hot leg path (He/LS IHX; PRF=10)

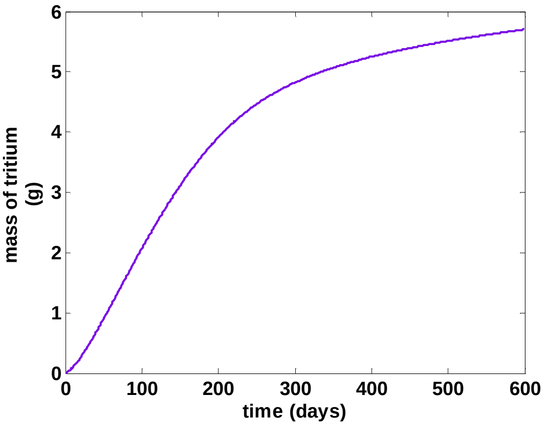

Fig. 19: Tritium mass which permeates through the hot leg path (He/LS IHX; PRF=10)

But, during the two first years, the activity of the produced hydrogen is still above the harmless limit (Fig.20).

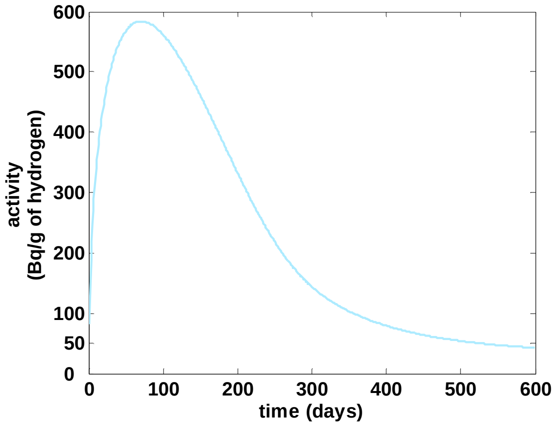

Fig. 20: Activity of hydrogen (Bq/g of H_2) by considering the hot leg path (He/LS IHX; PRF=10)

Therefore, the coupling with a tritium removal system in the primary coolant system is indispensable.

ii. AHTR

In the AHTR, if we consider the hot leg path, one year after the start-up of the reactor, the activity of tritium is below 10 Bq/g (Fig. 21). It corresponds to the harmless limit.

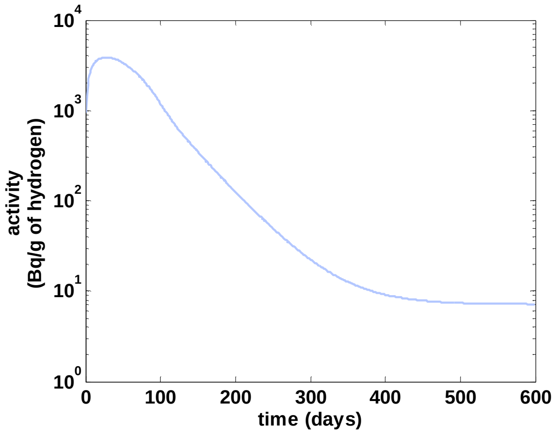

Fig. 21: Activity of hydrogen (Bq/g of H_2) by considering the hot leg path in the AHTR (PRF=10)

Therefore, in the AHTR, the hot leg path could be efficient. The reason is the relative high tritium partial pressure in the salt (~5000 Pa). Additional tritium recovery could occur with the primary salt cover gas system.

But we can notice that the activity of the hydrogen produced during the first year after the start-up of the reactor, still remains a potential issue.

4. Perspectives

The tritium transport study has shown that a tritium removal system is likely required if the tritium contamination of hydrogen is to be limited, with the assumption that the water resulting from hydrogen combustion is not diluted. We can determine its necessary efficiency. In the VHTR, to reach the harmless limit, the detritiation system has to maintain a tritium partial pressure of at least 0.2 Pa (in order to reduce the partial pressure by a factor 10 and thus, reduce the activity of hydrogen by a factor 100 which is 800 Bq/g with PRF=10). Some process could be used in the primary loop of the VHTR. The most common employs oxidation of tritiated gases in a catalytic recombiner and subsequent collection of HTO on molecular sieve dryers. But we don't know if this system would be sufficient and fast enough. Moreover, the addition of water in the coolant could cause oxidation issues. For the AHTR, where tritium would have a high partial pressure due to its low solubility in the primary coolant, the salt cover gas system may provide effective tritium removal and recovery.

The study of the hot leg path for the liquid salt intermediate fluid has shown that the hot leg may provide an efficient way to remove tritium from the reactor (especially for the AHTR). But it may be difficult to have a gas layer around the hot leg pipe.

Conclusions

The tritium transport study served multiple purposes:

First, it has been shown that some experimental data are necessary to calculate with low uncertainty the tritium inventory in the reactor. A better understanding of the tritium transport at the liquid salt/silicon carbide interface would be very useful. It would particularly be interesting to determine the order of magnitude of the permeation reduction factor at this interface.

In spite of the uncertainties, the order of magnitude of the hydrogen activity has been calculated. The silicon carbide used in the Process Heat Exchanger is a good permeation barrier but additional tritium transport control devices are necessary to reach the regulatory requirements.

Tritium removal system from gas could be adapted to the VHTR. In the AHTR, the hot leg path may be an efficient way to remove tritium from the reactor, as could tritium recovery from the primary salt cover gas.

Bibliography

[1] Tetsuaki Takeda, Jin Iwatsuki, Yoshiyuki Inagak "Permeability of hydrogen and deuterium of Hastelloy XR" Journal of Nuclear Materials 326 (2004) 47–58.

[2] Satoshi Fukada, Akio Morisaki, "Hydrogen permeability through a mixed molten salt of LiF, NaF and KF (Flinak) as a heat-transfer fluid", Journal of Nuclear Materials 358 (2006) 235–242.

[3] Rion A. Causey, William R. Wampler, The use of silicon carbide as a tritium permeation barrier, Journal of Nuclear Materials 220-222 (1995) 823-826.

[4] Blandine Laurenty, Per F. Peterson (Research Advisor), "The LM-LS experiment: investigating corrosion control, in Liquid Fluoride Salts, by Liquid alkali Metal", Report UCBTH-06-002 (M.S. Project Report).

[5] G. A. Esteban, A. Perujo, L. A. Sedano, F. Legarda, B. Mancinelli and K, Douglas, "Diffusive transport parameters and surface rate constants of deuterium in Incoloy 800", Journal of Nuclear Materials 300 (2002) 1–6.

[6] O. Serot, C. Wagemans, J. Heyse, "New results on helium and tritium gas production from ternary fission", AIP Conference Proceedings, May 24, 2005, Volume 769, pp. 857-860.

[7] Per F. Peterson, H. Zhao, and G. Fukuda, "Comparison of Molten Salt and High-Pressure Helium for the NGNP Intermediate Heat Transfer Fluid"**,** Report UCBTH-03-004.

[8] M. N. Chubarov, M. V. Krivosheev, "Behaviour of tritium released into the working rooms of the International Thermonuclear Experimental Reactor", Plasma Devices and Operations, Vol. 14, No. 3, September 2006, 201–213.

[9] H. Katsuta, K. Furukawa, "Diffusivity and solubility of hydrogen in molten fluoride mixture (LiF-NaF-KF)", Fusion Engineering and Design, Volume 81.

[10] Hirofumi Nakamura, Masataka Nishi, "Experimental evaluation of tritium permeation through stainless steel tubes of heat exchanger from primary to secondary water in ITER", Journal of Nuclear Materials 329–333 (2004) 183–187.

[11] Alain Griveau, Per Peterson (Research Advisor), "Modelling and Transient Analysis for the Pebble Bed Advanced High Temperature Reactor (PB-AHTR)", UCBTH-07-001 (M.S. Project Report).

[12] Massimiliano Fratoni, Ehud Greenspan, Per Peterson, "Neutronic and Depletion Analysis of the PB-AHTR", Paper Prepared for Global 2007: Advanced nuclear fuel cycle and systems, Boise, Idaho.

[13] Thermal Neutron Cross Sections: http://ie.lbl.gov/ngdata/sig.htm

[14] C. W. Forsberg, “Production of hydrogen using nuclear energy”, International Scientific Journal for Alternative Energy and Ecology, N°2 (10) (2004).

[15] C. W. Forsberg, P. F. Peterson, L. J. Ott, “The Advanced High-Temperature Reactor (AHTR) for Producing Hydrogen to Manufacture Liquid Fuels”, Paper Prepared for Rohsenow Symposium on Future Trends in Heat Transfer, MIT (2003).

[16] Tae-Keun Park, Seon-Ki Kim, “Tritium: its generation and pathways to the environment at CANDU 6 generating stations,” Nuclear Engineering and Design 163 (1996) 405–411.

Appendices

Appendix 1:

Thermophysical properties of primary coolants at their typical temperature of use

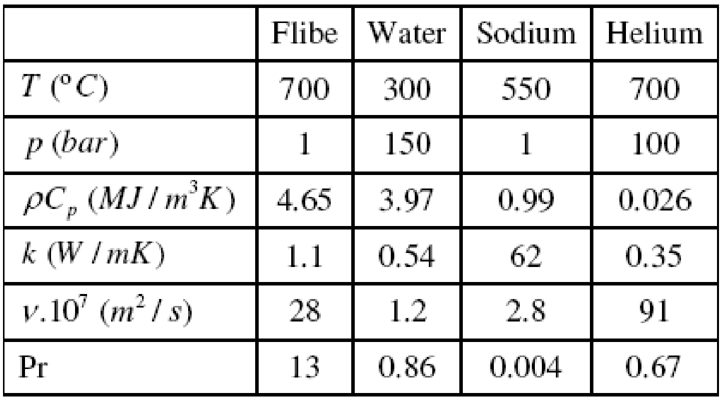

	Flibe	Water	Sodium	Helium
$T\ (^{o}C)$	700	300	550	700
$p\ (bar)$	1	150	1	100
$\rho C_p\ (MJ / m^3K)$	4.65	3.97	0.99	0.026
$k\ (W / mK)$	1.1	0.54	62	0.35
$\nu.10^7\ (m^2 / s)$	28	1.2	2.8	91
Pr	13	0.86	0.004	0.67

Appendix 2:

AHTR preconceptual design parameters

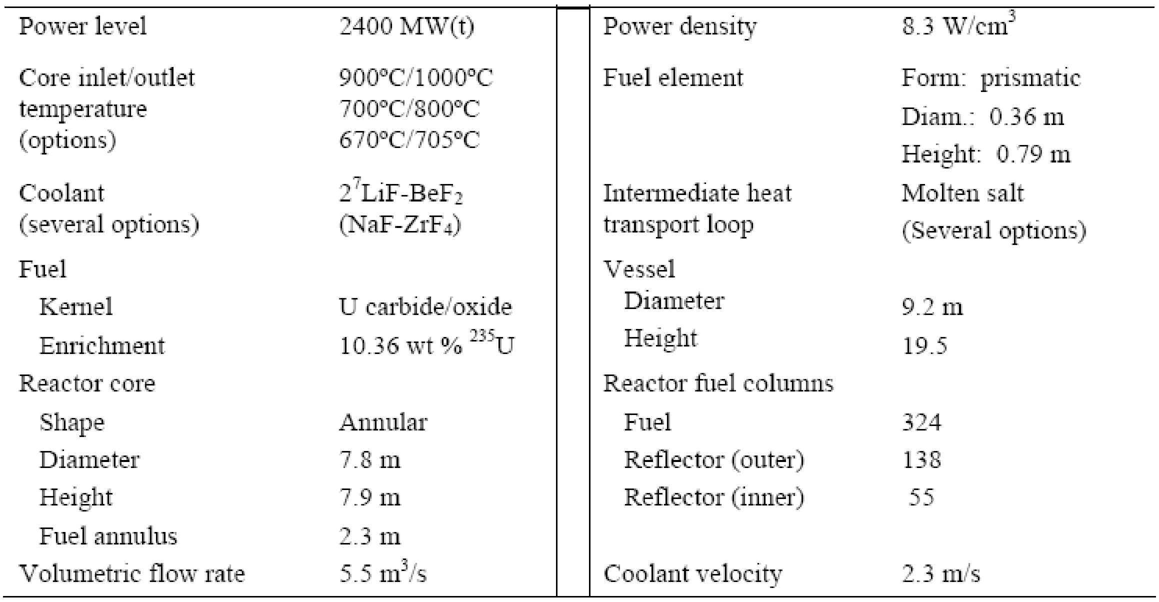

Power level	2400 MW(t)	Power density	8.3 W/cm^3
Core inlet/outlet temperature (options)	900°C/1000°C 700°C/800°C 670°C/705°C	Fuel element	Form: prismatic Diam.: 0.36 m Height: 0.79 m
Coolant (several options)	$2\,^{7}\text{LiF-BeF}_2$ (NaF-ZrF_4)	Intermediate heat transport loop	Molten salt (Several options)
Fuel		Vessel	
Kernel	U carbide/oxide	Diameter	9.2 m
Enrichment	10.36 wt % ^{235}U	Height	19.5
Reactor core		Reactor fuel columns	
Shape	Annular	Fuel	324
Diameter	7.8 m	Reflector (outer)	138
Height	7.9 m	Reflector (inner)	55
Fuel annulus	2.3 m		
Volumetric flow rate	5.5 m^3/s	Coolant velocity	2.3 m/s

Appendix 3:

Scaled comparison of the 600 MW_{th} GT-MHR reactor and the 2400 MW_{th} AHTR

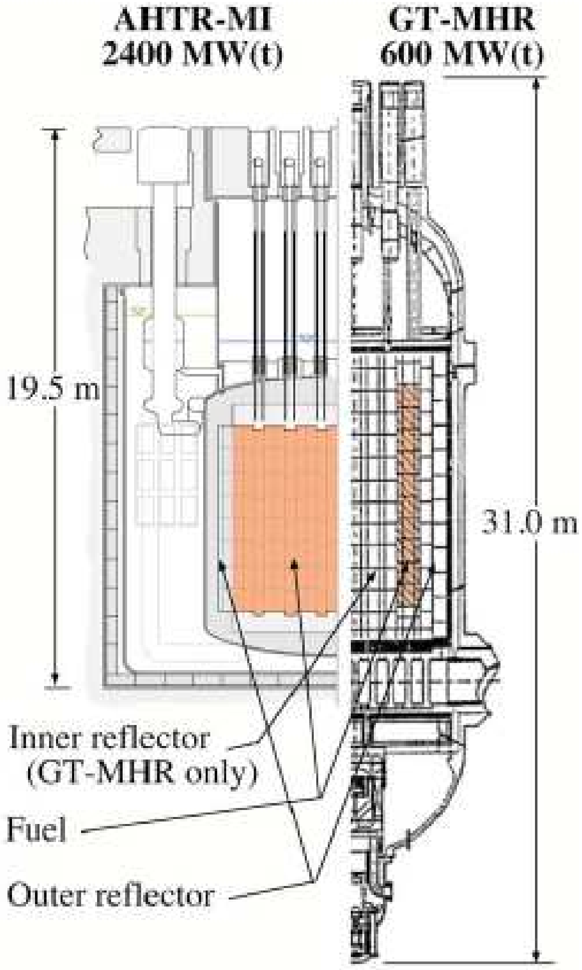

Appendix 4:

Comparison of 600 MW_{th} compact intermediate heat exchanger designs
(the molten salt is flinak)

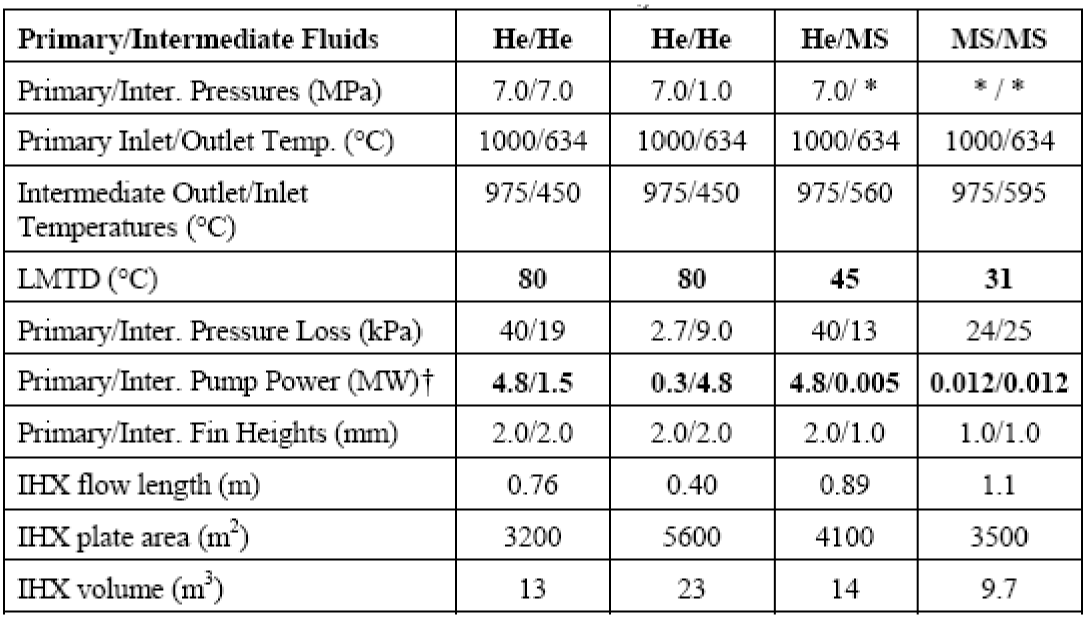

Primary/Intermediate Fluids	He/He	He/He	He/MS	MS/MS
Primary/Inter. Pressures (MPa)	7.0/7.0	7.0/1.0	7.0/ *	* / *
Primary Inlet/Outlet Temp. (°C)	1000/634	1000/634	1000/634	1000/634
Intermediate Outlet/Inlet Temperatures (°C)	975/450	975/450	975/560	975/595
LMTD (°C)	**80**	**80**	**45**	**31**
Primary/Inter. Pressure Loss (kPa)	40/19	2.7/9.0	40/13	24/25
Primary/Inter. Pump Power (MW)†	**4.8/1.5**	**0.3/4.8**	**4.8/0.005**	**0.012/0.012**
Primary/Inter. Fin Heights (mm)	2.0/2.0	2.0/2.0	2.0/1.0	1.0/1.0
IHX flow length (m)	0.76	0.40	0.89	1.1
IHX plate area (m^2)	3200	5600	4100	3500
IHX volume (m^3)	13	23	14	9.7

Appendix 5:

Matlab code for the modeling of the tritium transport in the VHTR with a He/LS IHX (the hot leg path is not considered)

```
clc;
clear;

Sigma=5.3e3; %barns
Phi=1.7*10^13; %cm-2.s-1 (neutron flux in the helium coolant)
m0=5;%g (initial amount of 4He)
mp=0.5/(3600*24*365.25); %g.s-1 (production rate by ternary fission)
S1=4100; %m2 (surface area of the exchanger)
Kxrt=(sqrt(2)*10^5/(sqrt(3)*8.314*273.15))*2.5e-8*exp(-76.6e3/(8.314*1273));
%mol.m-1.s-1.Pa-0.5 (t2)
Slsh=3.98e-7*exp((34.4e3)/(8.314*1273)); %mol.m-3.Pa-1 (h2)
V2=100; %m3
Ksict=2*10^(-15); %mol.m-1Pa-0.5 s-1 (t2?)

PRF1=10;% Permeation Reduction Factor
PRF2=10;

n1=1+24*3600e4;
n2=1+24*3600e2;

ms1(1)=0;
ms2(1)=0;
ms3(1)=0;
ps1(1)=0;
ps2(1)=0;
js1(1)=0;
js2(1)=0;

m1=0.001;
m2=0;
m3=0;
p1=0;
p2=0;
j1=0;
j2=0;
```

```
for i=2:3


    for j=2:n1

        mt=m0*(exp(-Sigma*10^(-24)*Phi*0.0001*((n1-1)*(i-2)+j-2))
        -exp(-Sigma*10^(-24)*Phi*0.0001*((n1-1)*(i-2)+j-1))); %g (tritium production)

        p1=m1/(m1+2*3*14.3e3*265/4)*7e6; %Pa (t2 partial pressure in the primary coolant)
        p2=m2/(2*V2*3*Slsh); %Pa (t2 partiam pressure in the secondary coolant)
        j1=2*Kxrt*(sqrt(p1)-sqrt(p2))/(PRF1*1.6*10^(-3)); %mol.m-2.s-1 (t flux through the
IHX)
        j2=2*Ksict*sqrt(p2)/(PRF2*1.6*10^(-3)); %mol.m-2.s-1 (t flux through the PHX)
        m3=m3+3*0.0001*S1*j2; %g (t hydrogen side)
        m2=m2+3*0.0001*S1*(j1-j2); %g (t secondary coolant)
        m1=m1+mt-3*0.0001*S1*j1; %g (t primary coolant)

    end

     ms1(i-1)=m1;
     ms2(i-1)=m2;
     ms3(i-1)=m3;
     ps1(i-1)=p1;
     ps2(i-1)=p2;
     js1(i-1)=j1;
     js2(i-1)=j2;

     i


end

for i=4:600


    for j=2:n2

        mt=m0*(exp(-Sigma*10^(-24)*Phi*0.01*((n2-1)*(i-2)+j-2))
        -exp(-Sigma*10^(-24)*Phi*0.01*((n2-1)*(i-2)+j-1))); %g (t)
        p1=m1/(m1+2*3*14.3e3*265/4)*7e6; %Pa (t2)
        p2=m2/(2*V2*3*Slsh); %Pa (t2)
        j1=2*Kxrt*(sqrt(p1)-sqrt(p2))/(PRF1*1.6*10^(-3)); %mol.m-2.s-1 (t)
        j2=2*Ksict*sqrt(p2)/(PRF2*1.6*10^(-3)); %mol.m-2.s-1 (t)
        m3=m3+3*0.01*S1*j2; %g (t)
        m2=m2+3*0.01*S1*(j1-j2); %g (t)
        m1=m1+0.01*mp+mt-3*0.01*S1*j1; %g (t)

    end
```

```
ms1(i-1)=m1;
     ms2(i-1)=m2;
     ms3(i-1)=m3;
     ps1(i-1)=p1;
     ps2(i-1)=p2;
     js1(i-1)=j1;
     js2(i-1)=j2;

     i


end


figure; plot(1:1:599,ms1,1:1:599,ms2,1:1:599,ms3);

ms4(1)=365*ms3(1)/(6e10);%g tritium/g of hydrogen
a(1)=(ms4(1)*1.83*6.02e14)/3;%Bq/g of hydrogen

for i=2:599
    ms4(i)=365*(ms3(i)-ms3(i-1))/(6e10);%g T/g H
    a(i)=1.83e-9*6.02e23*ms4(i)/3;%Bq/g H
end

figure; plot(1:1:599,a);
```